Impervious surface areas classification from GeoEye-1 satellite imagery using OBIA approach in a coastal area of Almeria (Spain)

Ismael, Fernández [(a)], Fernando J., Aguilar [(a)], Manuel A., Aguilar [(a)], Flor, Álvarez[(b)], María del Mar, Saldaña[(a)]

[(a)] Polytechnic High School and Faculty of Experimental Sciences, Department of Engineering. University of Almería, belonging to the CEI-MAR Campus of International Excellence ceiA3 (www.campusdelmar.es/).
[(b)] Technical and Superior School of Mining Engineering, Department of Mining Engineering, University of León.

Article Information

Keywords:
Remote Sensing
Object-Based Image Analysis
Support Vector Machine
Impervious Surface Area
GeoEye-1

Corresponding author:
Ismael Fernández
Tel.: +34950015997
Fax.: +34950015491
e-mail: ismaelf@ual.es
Address: Crta. de Sacramento s/n. La Cañada de San Urbano, 04120 Almería, Spain

Abstract

In order to map impervious surfaces for a coastal area using GeoEye-1 very high resolution (VHR) satellite imagery, an object-based image analysis (OBIA) approach has been performed. The non-parametric Support Vector Machine (SVM) classifier was applied to distinguish between two target classes: pervious and impervious. Moreover, different feature vectors were used to select the most appropriate set to achieve the highest accuracy as possible. Those feature sets combine i) basic information (spectral values of the red, green, blue, near-infrared, and panchromatic bands), ii) ratios between bands (red, green, and blue ratios, green/red ratio, and normalized difference indexes for red, green, and blue), and iii) texture information extracted through local variance computed at different window sizes (3x3, 5x5 and 7x7 pixels). The Kappa test was performed to check the statistically significant differences between all the feature sets and a separability matrix was constructed. Finally, the obtained accuracy results were compared with a similar experiment carried out on orthoimages from an archival photogrammetric flight which covered the same area. Statistically significant better accuracy results were provided by VHR satellite imagery when texture information was not included in the feature space. However, no differences were observed between both approaches when texture information was added.

1 Introduction

Impervious surface areas (ISAs) are defined as anthropogenic features thorough water cannot infiltrate into the soil [1] and they are a good indicator of the degree of urbanization in one area. ISAs influence the hydrology of the watershed, impacting on the runoff features and increasing the stormflow [2]. Thus, determination of ISA percentage is crucial for the evaluation of non-point runoff and the estimate of the water quality. Additionally, the percentage of ISA is correlated with the health of the ecosystem [3] which could be classified as stressed (up to 10% of the total area is ISA), impacted (between 11 and 25%), and degraded (more than 25%).

Remote sensing techniques constitute an efficient alternative to identify pervious/impervious surfaces. The development of the very high spatial resolution (VHR) satellite imagery has enabled a more detailed ISAs classification [4]. Platforms such as IKONOS, QuickBird, GeoEye-1 or WorldView-2 allow the application of classification approaches over fine spatial resolution images, with a ground sample distance from 1 meter and even better in their panchromatic bands (PAN). Moreover, those satellite imagery include some spectral bands, such us Near-Infrared (Nir), which can improve classification significantly if compared with archival aerial orthoimages, which are tipically composed by red, green, and blue (RGB) bands. That novelty make important to check the capability of the new satellite imagery for ISAs classification. In this sense, this work tests an object-based image analysis (OBIA) by a non-parametric classification approach on GeoEye-1 orthoimages over a coastal area of Almeria Spain.

OBIA approaches have been used since high spatial resolution imagery made difficult to classify scenes in which a higher local variance exists and pixel-based methods can lead to a “salt and pepper” effect [5]. In addition, urban environments are particularly difficult to classify since they consist of small features and very different materials which are all captured through the small ground sample distance (GSD). OBIA has been highlighted as an approach that can significantly improve the performance of supervised classifiers [6]. OBIA approaches are based on aggregating individual pixels in

order to obtain meaningful segments or objects according to some parameters. It also enables the use of additional information such as context, shape or texture.

The non-parametric methods allow avoiding the previous assumptions about the data distribution and, therefore, they are preferred for many applications. The non-parametric approach used in this work to classify the scene was the widely known Support Vector Machines (SVM) [7] which, in short, tries to find a hyperplane that splits a training data set into two subsets by using a minimum number of samples.

Another important issue is to select the most relevant feature set that leads to the best accuracy classification result. In this work, basic spectral information, indexes between bands and basic texture information are tested in order to find the most suitable feature set. The accuracy assessment and the Kappa test were carried out in order to determine the significant differences between the different feature sets and, therefore, statistically robust results were achieved. Furthermore, separability matrices were constructed in order to clarify the results.

The approach described here is based on a general methodology previously developed on an archival aerial orthoimage of the same area [8] and, therefore, the accuracy of both classifications, GeoEye-1 image and archival orthoimages, can be compared.

2 Study site

The study area comprises a heavily developed coastal area in Almería (Mediterranean Coast, South-East of Spain) between the villages of Villaricos and Garrucha (Fig. 1). The working area is approximately 11 km long and 775 m wide corresponding to the most urbanized area of that part of the coast. In order to compare the obtained results, the total area was divided in three zones in order to follow the same limits as in previous experiments on archival orthoimages [8] (Fig. 2): (1) pilot area in which all feature sets are tested, (2) area A in the north of the image, and (3) area B in the south.

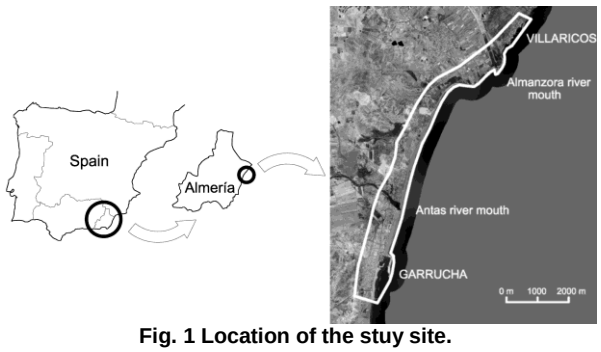

Fig. 1 Location of the stuy site.

3 GeoEye-1 Data

The original GSD for GeoEye-1 imagery at nadir is 0.41 m for PAN and 1.65 m at nadir for multispectral (MS), including the bands Red, Green, Blue, and Near Infrared (Nir). However, the final produces have to be down-sampled to 0.5 m and 2 m GSD for PAN and MS, respectively. For this work, a bundle of PAN and MS Geo images of GeoEye-1 taken in August, 2011, with an off-nadir angle of 9º was utilized. Two different orthoimages were generated from the original Geo images (PAN and MS) of GeoEye-1. One PAN orthoimage was performed using the rational polynomial coefficients (RPCs) refined with 7 accurate ground control points (GCPs) by means of a simple translation at the image space and a high accurate LIDAR-derived DEM. The final $RMSE_{2D}$, evaluated on 48 independent check points (ICPs) was 0.41 m. The second orthoimage was based on the pan-sharpened image with 0.5 m GSD and containing the spectral information gathered from the MS image (four bands). The pan-sharpened orthoimage was obtained with the same resolution and accuracy as for the PAN one. For further and detailed information, see the previous works [9]-[10].

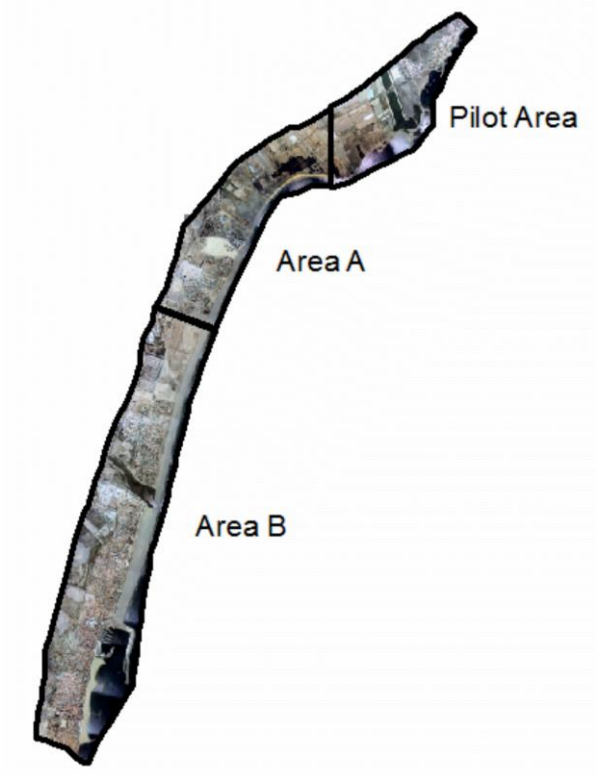

Fig.2 Distribution of the different experimental areas.

4 Methods

As previously mentioned, the classification of ISAs was carried out through a non-parametric classified applied over an OBIA approach. In order to be compared with a previous experiment developed on a very high resolution archival orthoimage [8]; the methodology used in this work follows the general conclusions and learning from that study (hereafter referred as ArO).

4.1 Minimum Classification Unit

The minimum classification unit was the segment or object, instead of pixel. It means that every object in the scene was classified as pervious or impervious, in accordance with the mean features values estimated with all pixels within the object. Accordingly, every training or validation sample corresponded only with one unique object. The segmentation was carried out through the multiresolution algorithm [11] implemented in eCognition 8 software. The segmentation process was performed over all bands included in both pan-sharpened and PAN orthoimages. The parameters shape and compactness were 0.3 and 0.7, respectively. In order to get a similar

number of objects than ArO experiment, a scale of 50 was chosen, and thus the objects size and meaning was similar.

4.2 Classification Strategy and Sampling

In the ArO experiment two strategies were taken into account: (1) aggregation, in which every different land use or class was identified (i.e. red buildings, pools, trees, and so on) and afterwards, each class was reclassified into pervious or impervious super-class; and (2) direct classification, in which, using the same samples, the super-classes pervious/impervious were targeted in one single step. The study demonstrated that both strategies lead to non-statistically different accuracy results and therefore, only direct classification has been considered for the present study.

Both, training and validation samples were extracted through a randomly stratified sampling method, based on the ArO study, being the collected samples as similar as possible to the earlier study, trying not to affect the accuracy results by differences in sampling. That means that the number of samples was similar as well as the location of samples and the number of sub-classes to be considered.

Summing up, 215 training and 728 validation well-distributed samples were collected for the pilot area, which was considered a suitable number of samples, according with [12].

4.3 Feature Sets Tested

The ArO study employed five different feature sets according with the information that they were composed: (1) only RGB information, (2) chromatic ratios added to RGB, (3) Grey Level Co-ocurrence Matrix (GLCM) texture added to both prior sets, (4) local variance added to 1 and 2 sets, and (5) all the prior features together. According with the accuracy results achieved by [8], GLCM was not considered for this work and the texture was only estimate by means of the local variance. Since the GSD of GeoEye-1 imagery was more than two times higher than the archival orthoimage (0.5 m for GeoEye-1 and 0.2 m for ArO); different window sizes were tested for this work. Thus, whereas only a 7x7 window was tested for the ArO study, covering an area of 9.8 m^2; 3x3, 5x5, and 7x7 window sizes were used for GeoEye-1 image (covering 4.5, 12.5, and 24.5 m^2).

Therefore, in order to compare the results of the present study with the ArO experiment, as well as estimate the most reliable feature set for GeoEye-1 imagery to classify ISAs, the sets are:

- RGB: only these three bands are considered to be able to be compared with the same ArO feature set (3 total features)
- Basic: PAN and Nir bands were added to RGB feature set (5 total features)
- Rates1: the same chromatic ratios than used in ArO were added to feature set 'Basic' in order to compare the results with ArO (9 total features)
- Rates2: the normalized differences for blue, green and red bands (NDBI, NDGI and NDVI, respectively) were considered and added to the feature set 'Rates1' (12 total features)
- Texture3: the local variance estimated through a 3x3 window size was added to the feature set 'Rates2' (13 total features)
- Texture5: the local variance estimated through a 5x5 window size was added to the feature set 'Rates2' (13 total features)
- Texture7: the local variance estimated through a 7x7 window size was added to the feature set 'Rates2' (13 total features)
- TextureAll: all the prior textures were added to the feature set 'Rates2' (15 total features)
- TextureOnly: all the window sizes textures were added to the feature set 'Basic' (8 total features)

4.4 Support Vector Machines

Opposite to the ArO study, in the present work only SVM was tested as a non-parametric classifier to identify ISAs. In the ArO study, other approaches such as Nearest Neighbour (NN) and Classification and Regression Trees (CART) were used for ISAs classification. For that experiment, CART was completely discarded according with the accuracy results, and NN yielded similar results to SVM but the first one resulted much more inefficient than the second one.

As previously mentioned, SVM method try to find a hyperplane which splits a data set into two subsets during the training phase, using a set of samples where the classification is previously known. The training phase tries to find the optimum boundary decision solution that minimizes misclassifications. It is important to highlight that not all samples are used to define the hyperplane but only those that are in the margin between classes are used for that. They are called the 'support vectors'. To obtain that hyperplane, a kernel function such as radial basic function (RBF) needs to be used. In the present work, as well as in the ArO study, the free-distribution library LIBSVM [13] was used for the application of SVM classifier.

4.5 Validation and Comparison

Error matrices for all feature sets were obtained and overall accuracy (OA), user's accuracy (UA), producer's accuracy (PA), KHAT statistic (K) and variance of K were derived from those error matrices (further information and formulation in [12]).

In order to compare between the results yielded by every feature set tested, the Kappa test (eq. 1) was used at a statistical level of significance $p < 0.05$.

$$Z_{12} = \frac{\left|\widehat{K}_1 - \widehat{K}_2\right|}{\sqrt{\widehat{var}\left(\widehat{K}_1\right) + \widehat{var}\left(\widehat{K}_2\right)}} \qquad (1)$$

Thus, if 1 and 2 represent two different error matrices, $\widehat{K}_1$ and $\widehat{K}_2$ are the KHAT statistic for each error matrix. KHAT statistic is standardized and normally distributed. Thus, the null hypothesis ($\widehat{K}_1 - \widehat{K}_2 = 0$) will be rejected if $Z_{12} \geq 1.96$ and the error would be considered significantly different at a 95% confidence level.

Therefore, comparison among K statistics obtained by all the feature sets will be useful to determine which feature set can be more appropriate for ISAs classification. Additionally, using the same kind of feature sets, the K values can identify the differences between the ArO study and the GeoEye-1 experiment by comparing both image sources with the same feature set.

4.6 Ad hoc vs. pilot area training for areas A and B

Similar to ArO experiment, three areas were separately classified in this work: pilot area, area A and area B (see Study Site section). The most suitable feature set that was found for the pilot area was also applied on areas A and B in two different ways. First, the pilot area training samples was utilized, extrapoling the support vectors to classify the areas A and B. Secondly, on-site training samples were acquired for both areas following the same randomly distributed strategy (*ad hoc* training) and then, the estimated support vectors were applied to classify the same area. Consequently, two sets of validation samples were also extracted for areas A and B. Thus, the exportability of the support vectors achieved for a pilot area and the influence of the working area can be tested.

Finally, all training samples from the three areas were joined in order to test the accuracy for the entire working area. The accuracy results were tested joining all the validation samples in one single validation set. Thus, two different strategies can be compared: (1) the pilot area training strategy, and (2) the entire area training strategy.

5 Results and Discussion

The attained results are shown according with the aim of the analysis: selection of the feature set that made the results more accurate, the classification results of the areas A and B using both pilot and *ad hoc* training sets, and the comparison between ArO experiment and GeoEye-1 results.

5.1 Selecting the most suitable feature set

The OA, PA, UA and KHAT results obtained through the error matrices for every feature set applied are shown in tab. 1.

Those results highlighted that all feature sets yielded accurate results since OA values exceeded the 85% considered as a minimum value for accurate according with [12] ranging from 86.8% to 90.0%. However, more differences were found for both UAs and especially for impervious PA (14.7% of differences between the maximum and minimum results). On one hand, the results implied that whereas the PA for the pervious class was very high, the PA results for the impervious class was significantly lower (the average of that difference was about 22%). On the other hand, the UA differences were much smaller (differences about 5%). That means that pervious class was classified more accurately, especially if omission error (related to PA) is considered. It is worth noting that PA was always higher than UA (about 9%) for pervious class, while UA was more accurate in all cases for impervious class (about 17%). In general, those results highlighted that impervious class was more difficult to classify than pervious class. This fact can be perfectly understandable since the impervious class is composed of a high number of different subclasses and materials, such as roads, buildings or paths.

The previous results shown that OA was not the most appropriate parameter to determine what feature set had to be chosen. In fact, all OA values seemed to be accurate results and they were not very different (from 86.3% to 90.0%). Otherwise, although the OA can be similar, the differences between the PA and UA for each class can also indicate the goodness of the accuracy results. For instance, whereas the 'Texture5' feature set has a similar OA than the 'TextureAll' set, the latter yielded much smaller differences regarding to PA and UA.

Feature set	OA	PA1	PA2	UA1	UA2	K
RGB	86.1	95.9	69.2	84.4	90.6	0.685
Basic	87.8	95.9	73.7	86.4	91.2	0.725
Rates1	86.8	97.2	68.8	84.4	93.4	0.699
Rates2	86.3	95.5	70.3	84.8	89.9	0.689
TextureOnly	87.4	93.5	76.7	87.4	87.2	0.720
Texture3	88.6	96.5	74.8	86.9	92.6	0.744
Texture5	88.9	97.2	74.4	86.8	93.8	0.749
Texture7	87.5	94.6	75.2	86.9	88.9	0.721
TextureAll	90.0	93.7	83.5	90.8	88.4	0.781

Tab. 1 General accuracy results. OA, PA and UA values in %. 1 and 2 indicate pervious and impervious class, respectively

Regarding to KHAT results, it is highlighted that every feature set yielded a good agreement and some of them were near to obtain strong agreement (>0.80 according to [12]). Those KHAT results were used to check the separability between the approaches through different Kappa tests which were grouping in a separability matrix (SM, see [8]) presented in tab. 2.

	TextureAll	Texture5	Texture3	Basic	Texture7	TextureOnly	Rates1	Rates2	RGB
TextureAll	0	0.91	1.05	1.55	1.65	1.68	**2.23**	**2.57**	**2.58**
Texture5	0.91	0	0.15	0.64	0.74	0.77	1.32	1.56	1.67
Texture3	1.05	0.15	0	0.49	0.60	0.62	1.18	1.41	1.52
Basic	1.55	0.64	0.49	0	0.10	0.13	0.68	0.92	1.03
Texture7	1.65	0.74	0.60	0.10	0	0.03	0.58	0.82	0.93
TextureOnly	1.68	0.77	0.62	0.13	0.03	0	0.55	0.79	0.90
Rates1	**2.23**	1.32	1.18	0.68	0.58	0.55	0	0.24	0.35
Rates2	**2.47**	1.56	1.41	0.92	0.82	0.79	0.24	0	0.11
RGB	**2.58**	1.67	1.52	1.03	0.93	0.90	0.35	0.11	0

Tab. 2 Separability matrix of KHAT values for GeoEye-1 feature sets. Values over 1.96 indicates significant differences for KHAT statistics (p<0.05)

The depicted SM highlighted that only 'TextureAll' feature set made the classification approach statistically different from others ('RGB', 'Rates1', and 'Rates2'). That contrasted with a previous study for a more reduced urban zone in the same area, in which the NDIs ratios achieved more accurate results than the basic feature set [14]. Additional features, such as the generated stereo-matching digital elevation model [15] was not included in order to compare accuracy results with the previous ArO experiment.

Summing up, only when all the available features used in this work were utilized, some differences could be estimated. Additionally, according with the low differences between PAs and UAs, 'TextureAll' feature set was chosen as the most suitable for ISAs classification by SVM approach.

5.2 Classifying A and B areas

According to the previous section, 'TextureAll' feature set was used to classify areas A and B for both pilot area and *ad hoc* training samples. The results are showed in a SM format in tab. 3.

		B_AH	A_AH	B_PI	A_PI
	KHAT	0.804	0.732	0.515	0.505
B_AH	0.804	0	1.84	**6.55**	**6.66**
A_AH	0.732	1.84	0	**4.67**	**4.81**
B_PA	0.515	**6.55**	**4.67**	0	0.20
A_PA	0.505	**6.66**	**4.81**	0.20	0

Tab. 3 Separability matrix for areas A and B classification using pilot area (PI) or ad hoc (AH) training samples

Some important variations in KHAT values can be seen in tab. 3. Whereas the KHAT statistic yield a good agreement for *ad hoc* training in both areas, the pilot area training leaded to inacurate results and can be considered as close to the poor agreement accuracy results (K<0.40 according with [12]). Regarding to the training samples, two different sections can be differenciated. First, *ad hoc* results are not significantly different each other, and second, the results from the pilot area training in areas A and B, which are also statistically similar each other. However, it is worth noting that the differences between *ad hoc* training and the pilot area training are really important and highlithed that a suitable design of the sampling method constitutes a key factor for image classification through this approach. Finally, it is important to note that, although no statistically significant, both *ad hoc* trainings yielded important differences and some additional test about the sampling method or the feature set could be taken into account.

5.3 Archival orthoimage accuracy vs GeoEye-1 accuracy

In order to check the influence of the source data for the proposed approach, the results obtained through ArO experiment were compared with those achieved by means of GeoEye-1 imagery. Three different feature sets were chosen for this comparison: 'RGB', 'Rates1', and 'TextureAll'. The comparison results (tab. 4) shown that 'RGB' and 'Rates1' feature sets for ArO were much more inaccurate than for GeoEye-1 experiment (GE). They also indicated that texture feature had an improvement effect for both studies but it was more important for ArO. Furthermore, the results for both experiments by means of 'TextureAll' feature sets yielded similar accuracy results. Therefore, a more reliable data source (VHR GeoEye-1 imagery) did not imply significant improvement if compared with results achieved from higher spatial resolution archival orthoimage which included some artefacts and had poor radiometry when texture features was applied. However, for basic information and ratios, the GeoEye-1 imagery yielded significantly higher accuracy, which could mean that this kind of images may have better radiometric conditions for image classification by not presenting any irregularity or artefacts that can be common for archival orthoimages.

This fact highlighted the importance of using invariable features, such as variance texture, for image classification. Moreover, it seems to be some limit on the classification accuracy around 90% of OA or 0.80 of KHAT inherent to the used approach. That could be related to the limitations of object-based analysis and therefore, under-segmentation errors could occur if the scale parameter was not the most appropriate for this images occur [16]. In fact, the experiment carried out by [16] through SVM classifier and OBIA approach over a QuickBird image obtained a maximum overall accuracy of about 90% for the most suitable scale parameter. In other work [17], a 92% OA when automatic classification was compared with air photo interpretation was achieved. However, the determination of the scale parameter which would lead to the most accurate classification was out of the scope of this work and a certain point of error due to image segmentation has to be taken into account.

	KHAT	Z statistic
GE_RGB	0.685	**4.11**
ArO_RGB	0.507	
GE_Rates1	0.699	**3.45**
ArO_Rates1	0.554	
GE_TextureAll	0.781	0.16
ArO_TextureAll	0.776	

Tab. 4 Separability results between ArO experiment and GeoEye-1 experiment (GE)

Other than the three different areas, the entire study site was classified using all the training samples and also all the validation samples of the three regions (pilot, A and B) through the 'TextureAll' feature set. The amount of samples was really high (583 training and 1783 validation samples) and the K statistic resulted in good agreement, as shown in tab. 5. In the same table, much smaller differences between PA and UA results can be tested and therefore, those differences seemed to be estabilized and the influence of the number and distribution of samples was also proved.

Additionally, the difference between both classifications was significantly different by applying the Kappa test ($p<0.05$) and the GeoEye-1 image was proved to yield more accurate results than the archival orthoimage.

Thus, the number and distribution of the samples was proved to be a key factor for classification accuracies. When a pilot area training was used to extrapolate the classification, the results were significantly more inaccurate than the cases in which local training were used. Moreover, a large amount of training and validation samples seemed to yield a more balanced results por PA and UA. Although out of the scope of this work, a more in deth study would be necessary to estimate the

appropriate sample size and distribution. Other works have concluded that non-parametric classifiers, such as SVM, can have different training size and distribution than the parametric methods in which the mean and variance of each class have to be sampled [18-19].

	GE	ArO
OA	90.4	88.1
PA1	90.5	88.6
PA2	90.1	87.5
UA1	91.5	89.2
UA2	89.0	86.8
KHAT	0.806	0.760

Tab. 5 Accuracy results por the entire area (pilot area + areas A and B). OA, PA and UA values in %. 1 and 2 indicate pervious and impervious class, respectively

6 Conclusion

The most suitable feature set for ISA classification from VHR GeoEye-1 PAN and pan-sharpened orthoimages was including texture feature, such as was previously proved for the same classification by archival orthoimages. Opposite to ArO experiment, basic and ratios-derived information achieved reasonable good-agreement, so the influence of the data source was demonstrated. It was also clear that the suitable accuracy results cannot be given only by the overall accuracy results and the balance between user's and producer's accuracy has to be taken into account as well.

Regarding to the pilot area and the *ad hoc* training sets, it was proved that the pilot area training results were not translatable to the other region and, similarly to the ArO study, the *ad hoc* training achieved a significant improvement for the accurate results. In this study, when the entire area was classified and all the training and validation samples were used, the GeoEye-1 classification was more accurate than that from ArO, although a good agreement was found for both experiments. Finally, a further study to test the size and distribution of sampling for the entire area could be necessary.

Acknowledgement

This work takes part of the general research lines promoted by the CEI-MAR Campus of International Excellence as a joint initiative between the universities of Almeria, Granada, Huelva and Málaga, headed by the University of Cádiz (further information can be retrieved from www.campusdelmar.es/). This work was supported by the Andalusia Regional Government, Spain, through the Excellence Research Project RNM-3575 and the Spanish Ministry for Science and Innovation (Spanish Government) under Grant Reference CTM2010-16573. Both projects are co-financed by the European Union through the European Regional Developed Funds (FEDER).

References

[1] Q. Weng. *Remote Sensing of impervious surfaces in the urban areas: Requirements, methods, and trends*. Remote Sensing of Environment 117, 15 (2012) pp 34-49.

[2] R.R. Gillies, J.B. Box, J. Symanzik and E.J. Rodemaker. *Effects or urbanization on the aquatic fauna of the Line Creek watershed, Atlanta-A satellite perspective.* Remote Sensing of Environment 86, 3 (2003) pp 411-422.

[3] C.L. Arnold and C.J. Gibbons. *Impervious surface coverage: The emergence of a key environmental indicator.* Journal of American Planning Association 62, 2 (1996) pp 243-258.

[4] D. Lu and Q. Weng. *Extraction of urban impervious surfaces from an IKONOS image.* International Journal of Remote Sensing 30, 5 (2009) pp 1297-1311.

[5] R. Pu, S. Landry and Q. Yu. *Object-based urban detailed land cover classification with high spatial resolution IKONOS imagery.* International Journal of Remote Sensing 32, 12 (2011) pp 3285-3308.

[6] T. Blaschke. *Object based image analysis for remote sensing*. ISPRS Journal of Photogrammetry and Remote Sensing 65, 1 (2010) pp 2-16.

[7] G. Mountakis, J. Im and C. Ogole. *Support Vector Machines in remote sensing: A review.* ISPRS Journal of Photogrammetry and Remote Sensing 66, 3 (2011) pp 247-259.

[8] I. Fernández, F.J. Aguilar, M.F. Álvarez and M.A. Aguilar. *Non-parametric object-based approaches to carry out ISA classification from archival aerial orthoimages*. IEEE Journal of selected topics in applied earth observations and remote sensing (*In press*)

[9] M.A. Aguilar, F.J. Aguilar, M. Saldaña and I. Fernández. *Geopositioning accuracy assessment of GeoEye-1 panchromatic and multispectral imagery.* Photogrammetric Engineering and Remote Sensing 78, 3 (2012) pp 247-257.

[10] M.A. Aguilar, M.M. Saldaña and F.J. Aguilar. *Assessing geometric accuracy of the orthorectification process from GeoEye-1 and WorldView-2 panchromatic images.* International Journal of Applied Earth Observation and Geoinformation 21, 1 (2013) pp 427-435.

[11] U.C. Benz, P. Hofmann, G. Willhauck, I. Lingenfelder and M. Heynen. *Multi-resolution object-oriented fuzzy analysis of remote sensing data for GIS-ready information.* ISPRS Journal of Photogrammetry and Remote Sensing 58, 3-4 (2004) PP 239-258.

[12] R.G. Congalton and K. Green. Assessing the accuracy of Remotely Sensed Data. Boca Raton 2009.

[13] C. Chang and C. Lin. *LIBSVM: A library for support vector machines*. ACM Transactions on Intelligent Systems and Technology 2 (2011).

[14] M.A. Aguilar, M.M. Saldaña and F.J. Aguilar. *GeoEye-1 and WorldView-2 pan-sharpened imagery for object-based classification in urban environments*.

International Journal of Remote Sensing 34, 7 (2013) pp 2583-2606.

[15] M.A. Aguilar, M.M. Saldaña and F.J. Aguilar. *Generation and quality assessment of stereo-extracted DSM from GeoEye-1 and WorldView-2 imagery*. IEEE Transactions on Geoscience and Remote Sensing (In Press).

[16] D. Liu and F. Xia. *Assessing object-based classification: advantages and limitations*. Remote Sensing Letters 1, 4 (2010) pp 187-194.

[17] M. Kampouraki, G.A. Wood and T.R. Brewer. *Opportunities and limitations of object based image analysis for detecting urban impervious and vegetated surfaces using true-color aerial photography.* In Object-based image analysis-Spatial concepts for knowledge-driven remote sensing applications, Springer-Verlag 2008 pp 555-569.

[18] G.M. Foody, A. Mathur, C. Sánchez-Hernández and D.S. Boyd. *Training set size requirements for the classification of a specific class*. Remote Sensing of Environment 104, 1 (2006) pp 1-14.

[19] G.M. Foody and A. Mathur. *Toward intelligent training of supervised image classifications: Directing training data acquisition for SVM classification.* Remote Sensing of Environment 93, 1-2 (2004) pp 107-117.